Heterogeneous uptake of carbonyl sulfide onto kaolinite within a temperature range of 220–330 K

Yongchun Liu,[1] Jinzhu Ma,[1] Chang Liu,[1] and Hong He[1]

[1]   In this study the heterogeneous uptake of carbonyl sulfide (OCS) onto kaolinite was investigated using a Knudsen cell reactor within the temperature range of 220–330 K. Results showed that OCS could only be adsorbed at Al-OH sites on kaolinite reversibly within this temperature region. The initial true uptake coefficient was measured to be $(1.68 \pm 0.12) \times 10^{-7}$ at 300 K. It showed no observable dependence on the pressure of OCS, while it varied significantly with temperature, and can be expressed as $\gamma_t = \exp(1293/T - 20.0)/[1 + \exp(1293/T - 20.0]$. The values of ΔH_{obs} and ΔS_{obs} during the adsorption process were -10.7 ± 1.1 kJ mol^{-1} and -166.3 ± 4.5 J K^{-1} mol^{-1}, respectively. The activation energy for desorption of OCS on kaolinite was 19.5 ± 1.1 kJ mol^{-1}. The uptake of OCS by kaolinite owing to reversible physisorption may have little influence on the sink of OCS in the atmosphere.

1. Introduction

[2]   Carbonyl sulfide (OCS) is the most abundant sulfur compound in the atmosphere, with a rather uniform mixing ratio of about 500 pptv in the troposphere [*Watts*, 2000]. Historically, it was regarded as the major source of stratospheric sulfate aerosol, which has an important influence on the Earth's radiation balance [*Crutzen*, 1976; *Turco et al.*, 1980] and stratospheric ozone chemistry [*Simmons et al.*, 1999]. Therefore, significant attention has been paid to the sources and sinks of OCS in the atmosphere.

[3]   To date numerous sinks have been identified, such as uptake by oxic soils and vegetation, consumption by reactions with OH and O, and direct photolysis [*Watts*, 2000]. Additionally, a few studies have reported that heterogeneous hydrolysis and oxidation reactions of OCS can take place on atmospheric particles, as well as model oxides such as Al_2O_3, SiO_2, Fe_2O_3, CaO, and MnO_2 [*Wu et al.*, 2004, 2005; *He et al.*, 2005; *Liu et al.*, 2006; *Y. Liu et al.*, 2007; *Liu and He*, 2008; *Chen et al.*, 2007]. For example, hydrogen thiocarbonate ($HSCO_2^-$) was observed as a key intermediate [*He et al.*, 2005; *Liu et al.*, 2006; *Y. Liu et al.*, 2007; *Liu et al.*, 2009]; H_2S and CO_2 were found to be gaseous products [*Y. Liu et al.*, 2007; *Liu and He*, 2008, 2009]; and sulfate, sulfite [*He et al.*, 2005; *Liu et al.*, 2006], and elemental sulfur [*Wu et al.*, 2004, 2005] were also observed as surface products. We recently further investigated the reaction kinetics of OCS on α-Al_2O_3, γ-Al_2O_3 [*Liu et al.*, 2008], and MgO [*Liu and He*, 2008; *Liu et al.*, 2009]. According

to the true uptake coefficients of OCS on α-Al_2O_3, the average dust loading in the troposphere, and the fraction of alumina in the mineral dust, the sink of OCS owing to heterogeneous reaction on mineral oxides was estimated to be 0.10 ± 0.02 Tg yr^{-1} [*Liu et al.*, 2008]. These results demonstrate that consumption of OCS by heterogeneous reactions on mineral dust might be equivalent to that reacting with OH [*Watts*, 2000] and might be a new sink of OCS in the troposphere.

[4]   It should be noted that single-component model oxides were used in most of these previous studies, which are similar to the common cases for heterogeneous reaction studies for SO_2, NO_2, N_2O_5, O_3, and HNO_3 on mineral oxides [*Dentener et al.*, 1996; *Andreae and Crutzen*, 1997; *Jacob*, 2000; *Underwood et al.*, 2000; *Usher et al.*, 2003]. Laboratory experiments, however, routinely indicate that the mineral composition greatly affects heterogeneous reactions and their corresponding uptake coefficients [*Hanisch and Crowley*, 2001; *Usher et al.*, 2003; *Angelini et al.*, 2007]. We also observed distinct differences in the uptake coefficients of OCS among MgO, α-Al_2O_3, and γ-Al_2O_3 [*Liu and He*, 2008; *Liu et al.*, 2008, 2009] It is necessary, therefore, to investigate reaction kinetics on other relevant atmospheric particles to accurately understand the sinks of OCS related to heterogeneous reactions.

[5]   Kaolinite clays, which are formed primarily through the chemical weathering of silicate rocks in arid regions, are generally fine-mode particles and common components of stratospheric micrometeorites [*Greshake et al.*, 1998; *Hatch et al.*, 2008]. Compared to coarse-mode particles (single-component oxides) with faster rates of gravitational settling, kaolinite clays undergoing long-range transport may have a greater influence on the sink of OCS. Additionally, soils have been considered to be important in the sinks and sources of OCS in the atmosphere [*Kesselmeier et al.*, 1999; *Watts*,

---

[1]State Key Laboratory of Environmental Chemistry and Ecotoxicology, Research Center for Eco-Environmental Sciences, Chinese Academy of Sciences, Beijing, China.

2000; *Kettle et al.*, 2002; *J. Liu et al.*, 2007]. Kaolinite can also be used as a real or model soil sample. Thus, it is also helpful for understanding the chemical processes of OCS in soils to investigate the heterogeneous uptake of OCS onto kaolinite. In this study the heterogeneous reaction of OCS on kaolinite was investigated using a Knudsen cell reactor and in situ diffuse reflectance infrared Fourier transform spectroscopy (DRIFTS). Uptake coefficients within a temperature range of 220–330 K were measured.

2. Materials and Methods

2.1. Materials

[6] The kaolinite sample originated from Anhui province, China, and was supplied by Huaibei Junteng Kaolinite Co., Ltd. Its specific surface area was measured to be 12.4 $m^2 g^{-1}$ using a Quantachrome Autosorb-1-C instrument. SiO_2, with a specific surface area of 4.8 $m^2 g^{-1}$, was suplied by Beijing Yili Fine Chemicals Co. Ltd. The α-Al_2O_3 sample, with a specific surface area of 12.0 $m^2 g^{-1}$, was prepared by calcining boehmite (AlOOH; supplied by Shandong Alumina Corporation) at 1473 K.

[7] All other chemicals were used as received, without further treatment. These included OCS (1.98%; OCS/N_2; Beijing Huayuan Gases Inc.), N_2 and O_2 (99.99% purity; Beijing AP BEIFEN Gases Inc.), and C_2H_5OH (99.7%, Beijing Chemicals Factory).

2.2. Experimental Methods

[8] A Knudsen cell reactor coupled to a quadrupole mass spectrometer (KCMS; Hiden, HAL 3F PIC) was used to measure the uptake coefficients of OCS onto kaolinite. The apparatus has been described in detail elsewhere [*Liu and He*, 2008; *Liu et al.*, 2008, 2009]. Briefly, the mass spectrometer was housed in a vacuum chamber equipped with a 300 L s^{-1} turbomolecular pump (Pfeiffer) and an ion gauge (BOC Edward). The vacuum chamber between the quadrupole mass spectrometer (QMS) and the Knudsen cell reactor was pumped by a 60 L s^{-1} turbomolecular pump for differential pumping of the mass spectrometer and ion gauge (both from BOC Edward). The Knudsen cell reactor consisted of a stainless-steel chamber with a gas inlet controlled by a leak valve, an escape aperture whose area could be modified with an adjustable iris, and a sample holder attached to the top ceiling of a circulating fluid bath. The area of the escape aperture was approximately 0.5 mm^2 and measured in each experiment according to the methods reported in our previous works [*Liu and He*, 2008; *Liu et al.*, 2008, 2009]. The sample in the sample holder can be exposed to or isolated from the reactants by a lid connected to a linear translator. The temperature of the sample holder was measured with an embedded Pt resistance thermometer and controlled from 220 to 373 K within ± 0.10 K using a superthermostat and cryofluid pump (DFY-5/80; Henan Yuhua Laboratory Instruments Co., Ltd.).

[9] Powder samples were dispersed evenly on the sample holder with ethanol and then dried at 393 K for 2 h. Pretreated samples and the reactor chamber were evacuated at 353 K for 6 h to reach a base pressure of approximately 5.0×10^{-7} Torr. After the system was cooled to the desired temperature, the sample cover was closed. Then 1.51% OCS gas, balanced with simulated air (21% O_2 and 79% N_2), was introduced into the reactor chamber through the leak valve. The pressure in the reactor was controlled with the leak valve and measured using the absolute pressure transducer. Prior to the experiments the reactor chamber was passivated with OCS in air for 150 min until a steady-state QMS signal was established as the oxide samples were isolated from the gas by the sample cover. Uptake coefficients were calculated based on the KCMS signal. According to the pressure in the vacuum chamber and the pumping speeds of turbomolecular pumps, the mass signal intensity of OCS could be converted to the flow rate of molecules into the reactor.

[10] In situ DRIFTS spectra were recorded on a NEXUS 670 (Thermo Nicolet Instrument Corp.) Fourier transfer infrared (FTIR) spectroscope, which was equipped with an in situ diffuse reflection chamber and a high-sensitivity mercury cadmium telluride (MCT) detector cooled by liquid N_2. IR spectra were collected and analyzed by a computer with OMNIC 6.0 software. All spectra reported here were recorded at a resolution of 4 cm^{-1} for 100 scans. A powder sample (about 10 mg) was finely ground and placed in a ceramic crucible in the in situ chamber. Before the DRIFTS measurement the sample was pretreated in the in situ reactor chamber at 393 K in a 100 mL min^{-1} simulated air stream (79% N_2 and 21% O_2) for 2 h. After the pretreated sample was cooled to 300 K in simulated air, the reference spectrum was collected. Then 1000 ppmv of COS balanced with simulated air was introduced into the reactor. Infrared spectra in the closed system were collected automatically by a computer.

3. Results and Discussion

3.1. Overview Uptake Behavior of Carbonyl Sulfide (OCS) Onto Kaolinite

[11] Figure 1a shows the typical uptake curves of OCS onto kaolinite. This experiment was performed at 300 K with 181.2 mg of kaolinite. The average OCS partial pressure in the Knudsen cell reactor was $(5.3 \pm 0.3) \times 10^{-6}$ Torr, which is equivalent to $(1.7 \pm 0.2) \times 10^{11}$ mol cm^{-3} or 7.0 ± 0.2 ppbv in the atmosphere. The QMS signal of OCS ($m/e = 60$) decreased dramatically after the sample cover was opened (Figure 1a). With an increase in exposure time, the QMS signal of OCS increased gradually owing to the saturation adsorption of OCS onto the surface. After the sample was exposed for approximately 15 min, the QMS signal of OCS recovered to its baseline. Besides OCS, other mass channels, including CO_2 ($m/e = 44$) and H_2S ($m/e = 34$), were monitored synchronously during the uptake experiment. However, desorption of CO_2 and H_2S was not observed (not shown). These phenomena are much different from those taking place on Al_2O_3 and MgO, in which a steady-state consumption of OCS accompanied by CO_2 and H_2S formation due to hydrolysis reaction is observed [*Liu and He*, 2008; *Liu et al.*, 2008, 2009]. These results suggest that only adsorption of OCS was taking place on kaolinite in this study.

[12] Additionally, when the uptake experiment was finished, the sample cover was closed and the reactant gas disappeared. After the QMS signal became steady, desorption of OCS was observed prominently when the sample cover was opened again, with the same area of escape aperture (Figure 1a). For Al_2O_3 and MgO samples, however, no
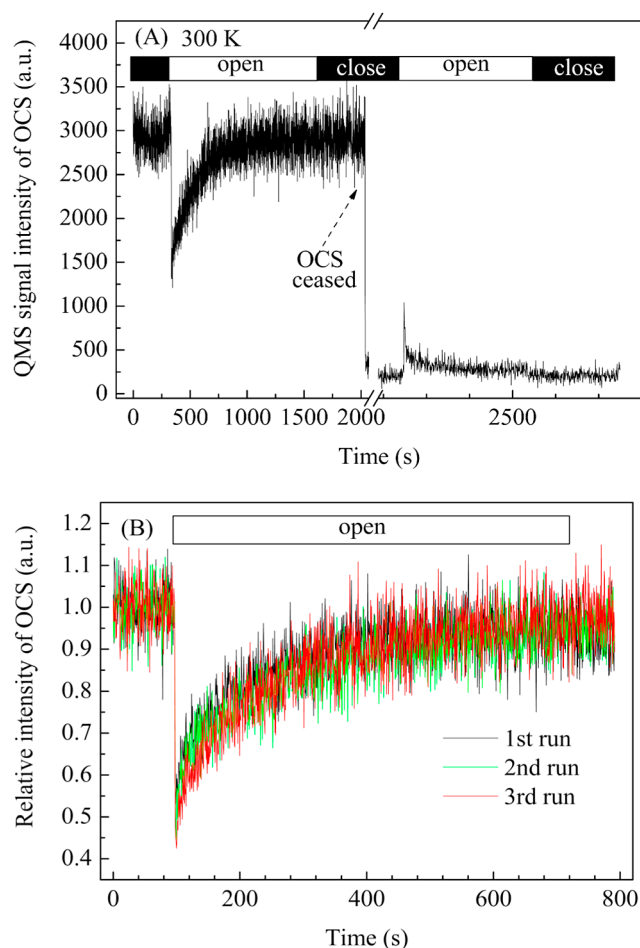
Figure 1. Uptake curves of carbonyl sulfide (OCS) on 181.2 mg of kaolinite at 300 K and at $(5.3 \pm 0.3) \times 10^{-6}$ Torr. (a) Adsorption and desorption curves; (b) repeated uptake curves at 300 K for the same sample after being evacuated at 353 K for 6 h with a base pressure of $\sim 5.0 \times 10^{-7}$ Torr.

desorption of OCS was observed even when the escape aperture area was increased to 2.73 cm^2 (maximal value of the iris) from 0.5 mm^2 (the value used in the uptake experiments) [*Liu and He*, 2008; *Liu et al.*, 2008]. The preceding results indicate that OCS adsorbs onto kaolinite reversibly. However, only about 12% of OCS desorbed from the surface at this temperature, according to the integrated area of adsorbed and desorbed OCS. After the reacted sample was re-evacuated at 353 K and 5.0×10^{-7} Torr for 6 h, repeated uptake experiments under the same conditions were performed. As shown in Figure 1b the uptake curves for the second and third runs coincided well with that for the first run. These results indicate that a portion of OCS can reversibly adsorb onto kaolinite at 300 K, and the remaining part can also desorb at higher temperatures (353 K). We also carried out desorption experiments at other temperatures after the uptake experiments. The proportion of reversible adsorption for OCS was measured to be 34% at 273 K and 50% at 238 K, which means that more sites with less activity contributed to adsorption of OCS onto kaolinite at lower temperatures.

[13] In our previous work we have confirmed that surface OH is the reactive site for the heterogeneous reaction or adsorption of OCS on mineral oxides [*Liu and He*, 2009; *Liu et al.*, 2006; *J. Liu et al.*, 2007; *Y. Liu et al.*, 2007; *Liu et al.*, 2009]. Kaolinite is a type of aluminum phyllosilicate mineral with the empirical formula $Al_2Si_2O_5(OH)_4$, indicating that there are two types of adsorption sites (Al and Si sites) for OCS on the surface of kaolinite. To clarify which one was active in OCS adsorption, uptake experiments under the same reaction conditions on kaolinite were performed on 71.0 mg of α-Al_2O_3 and 350.5 mg of SiO_2, respectively. The uptake curves are shown in Figure 2. As shown in Figure 2a the uptake of OCS on α-Al_2O_3 was very clear, although its surface area in this experiment was lower than that of kaolinite (Figure 1a). This phenomenon was the same as our previous results [*Liu et al.*, 2008]. No observable uptake of OCS took place on SiO_2 (Figure 2b), however, even though its surface area was close to that of kaolinite. Therefore, uptake of OCS on kaolinite can be ascribed to Al-OH sites. Although both α-Al_2O_3 and kaolinite provide Al-OH sites, the heterogeneous processes of OCS on them are quite different. As reported previously, catalytic hydrolysis and oxidation reactions can occur on α-Al_2O_3, while no reactions take place on kaolinite. In situ DRIFTS spectra (shown in Figure 3) also confirmed the different reactivities of OCS on α-Al_2O_3 and kaolinite. Surface species including H_2CO_3 (1683 cm^{-1}), HCO_3^- (3623 and 1635 cm^{-1}), $HSCO_2^-$ (1578 cm^{-1}), and SO_4^{2-} (1384 cm^{-1}) [*Liu et al.*, 2009] were observed very clearly on α-Al_2O_3, while the intensity of these species on kaolinite was very weak. Particularly, gaseous CO_2 (2363 and 2338 cm^{-1}) formed when α-Al_2O_3 was exposed to OCS (2071 and 2052 cm^{-1}), while it did not occur on kaolinite under the same conditions. This difference in heterogeneous processes can be ascribed to the increase in surface acidity of Al-OH sites caused by the neighboring Si atoms in kaolinite [*Parry*, 1963] because a stronger basicity is favored in these reactions [*Liu et al.*, 2009]. The pH value of the slurry for 1.0 g α-Al_2O_3 in 20.0 mL water was measured to be 9.1, while that for kaolinite was 6.7.

3.2. Uptake Coefficient of OCS Onto Kaolinite at 300 K

[14] On the basis of the changes in QMS signal in a steady-state flow, the observed heterogeneous uptake coefficient (γ_{obs}), which represents the upper limit for the coefficient of uptake of gas by particles, can be calculated using the Knudsen cell equation [*Tabor et al.*, 1994; *Beichert and Finlayson-Pitts*, 1996; *Underwood et al.*, 2000; *Ullerstam et al.*, 2003; *Liu and He*, 2008; *Liu et al.*, 2008, 2009]:

$$\gamma_{obs} = \frac{A_h}{A_s} \frac{(I_0 - I)}{I} \qquad (1)$$

where A_h is the effective area of the escape aperture (cm^2) and was about 0.5 mm^2 measured in each experiment according to methods in our previous works [*Liu and He*, 2008; *Liu et al.*, 2008, 2009]; A_s is the geometric area of the sample holder (cm^2); and I_0 and I are the mass spectral intensities with the sample holder closed and open, respectively.

[15] Figure 4a shows the typical γ_{obs} values changing with exposure time. For an 181.2 mg kaolinite sample the initial observed uptake coefficient for the maximal value γ_{max} was
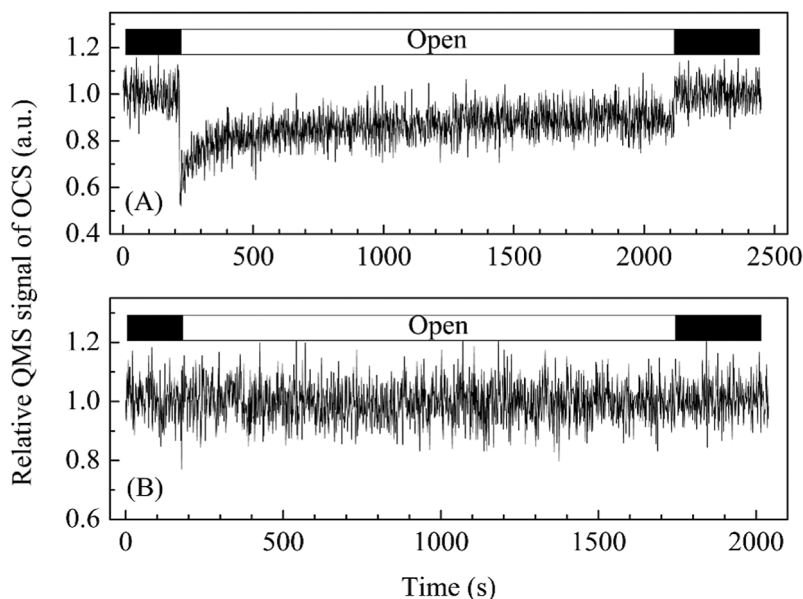
Figure 2. Uptake curves of OCS (a) on 71.0 mg of α-Al$_2$O$_3$ and (b) on 350.5 mg of SiO$_2$ at 300 K.

1.02×10^{-3}. With an increase in exposure time, it gradually decreased, eventually reaching 0 at steady state, which corresponded to the increase in the QMS signals of OCS. As shown in Figure 4a, γ_{obs} shows a high uncertainty owing to the noise of the mass spectrometer detector. Therefore, it is hard to determine the real initial observed uptake coefficient from the γ_{max} value. As shown in the inset in Figure 4a, the inverse γ_{obs} versus time shows a good linear relationship ($r = 0.81$). Therefore, the initial uptake coefficient (γ_0) was extrapolated from the intercept of the plot of γ_{obs} versus time. The corresponding γ_0 was measured to be $(8.51 \pm 0.51) \times 10^{-4}$.

[16] Because the reactant molecules can diffuse into the underlying layers of multilayer powder samples, the γ_{max} and γ_0 values increased linearly with the sample mass, then reached a knee point, followed by a constant value, as shown in Figures 4b and 4c. The error bars show a relative error of $\pm15\%$ measured by three reproducible experiments. This linear dependence between observed uptake coefficient and sample mass was also observed for the other reaction systems [Al-Abadleh and Grassian, 2000; Gebel and Finlayson-Pitts, 2001; Underwood et al., 2001; Ullerstam et al., 2003; Frinak et al., 2004; Liu and He, 2008; Liu et al., 2008, 2009]. The slopes for the plots in the region from 0 to 200 mg in Figures 4b and 4c are $(5.19 \pm 0.14) \times 10^{-6}$ mg^{-1} and $(4.48 \pm 0.10) \times 10^{-6}$ mg^{-1}, respectively. Therefore, the true uptake coefficient, γ_t, which represents the lower limit for the uptake coefficient, can be calculated from

$$\gamma_t = \text{slope}\left(\frac{A_s}{S_{BET}}\right) \qquad (2)$$

where slope is the slope of the plot of γ_{obs} versus sample mass in the linear regime (mg^{-1}), A_s is the geometric area (cm^2) of the sample holder, and S_{BET} is the specific surface area of the particle sample (cm^2 mg^{-1}) [Carlos-Cuellar et al., 2003; Liu and He, 2008; Liu et al., 2008, 2009]. The γ_t value

for OCS on kaolinite at 300 K and 5.3×10^{-6} Torr was measured to be $(2.11 \pm 0.06) \times 10^{-7}$ according to the slope of the plot of γ_{max} versus sample mass. The corresponding γ_t value according to the plot of γ_0 versus sample mass was $(1.82 \pm 0.04) \times 10^{-7}$.

[17] Figure 5 shows the changes in γ_t with the pressure of OCS (P_{OCS}) in the reactor from 9.9×10^{-7} Torr (corresponding to 1.3 ppb) to 6.3×10^{-6} Torr (corresponding to 8.3 ppb) at 300 K. The lowest P_{OCS} in this study was still higher than that in the real atmosphere (about 3.8×10^{-7} Torr), owing to the sensitivity limit of the mass spectrometer. As shown in Figure 5 the γ_t values showed no observable pressure dependence within the experimental uncertainties. This indicates that many more sites were accessible than just the necessary adsorption sites and, also,
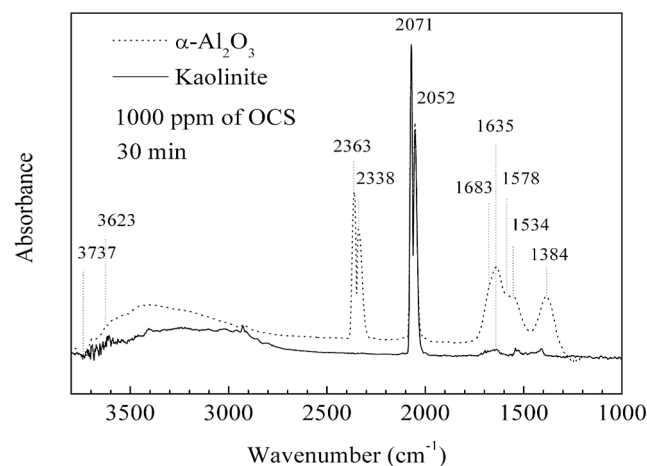

Figure 3. In situ diffuse reflectance infrared Fourier transform spectroscopy (DRIFTS) spectra for α-Al$_2$O$_3$ and kaolinite exposed to an air flow of 1000 ppm OCS at 300 K.

Figure 5. Effect of OCS pressure or concentration in the reactor on uptake coefficients at 300 K. Squares and triangles represent γ_t values calculated based on γ_{max} and γ_0, respectively.

recommend the initial true uptake coefficient of OCS on kaolinite at 300 K to be $(1.68 \pm 0.12) \times 10^{-7}$. In our previous studies [*Liu and He*, 2008; *Liu et al.*, 2008, 2009], the initial true uptake coefficients of OCS on α-Al_2O_3 and MgO under the same reaction conditions were measured to be $(3.80 \pm 0.80) \times 10^{-7}$ and $(4.84 \pm 0.60) \times 10^{-7}$, respectively. Thus, the γ_t value of OCS on kaolinite is less than about one-half of those on α-Al_2O_3 and MgO.

3.3. Effect of Temperature on Uptake of OCS Onto Kaolinite

[18] The temperature in the atmosphere varies with latitude, longitude, and altitude above the Earth's surface, as well as with season and time of day. For example, the tropospheric temperature for latitude 40°N during June decreases from room temperature (r.t.) to 220 K with an increase in altitude. In reality, the temperature at the tropopause can reach values much lower than 220 K, down to 180 K above the Antarctic in winter [*Smith*, 2003]. Therefore, the temperature dependence for the uptake coefficients of OCS on kaolinite was further investigated in the temperature region of 220–330 K.

[19] Table 1 lists the uptake coefficients and desorption rate constants (k_{des}) measured at different temperatures. The pressure of OCS in the reactor was $(5.3 \pm 0.3) \times 10^{-6}$ Torr and the sample mass was 181.2 mg. As reported in Table 1,
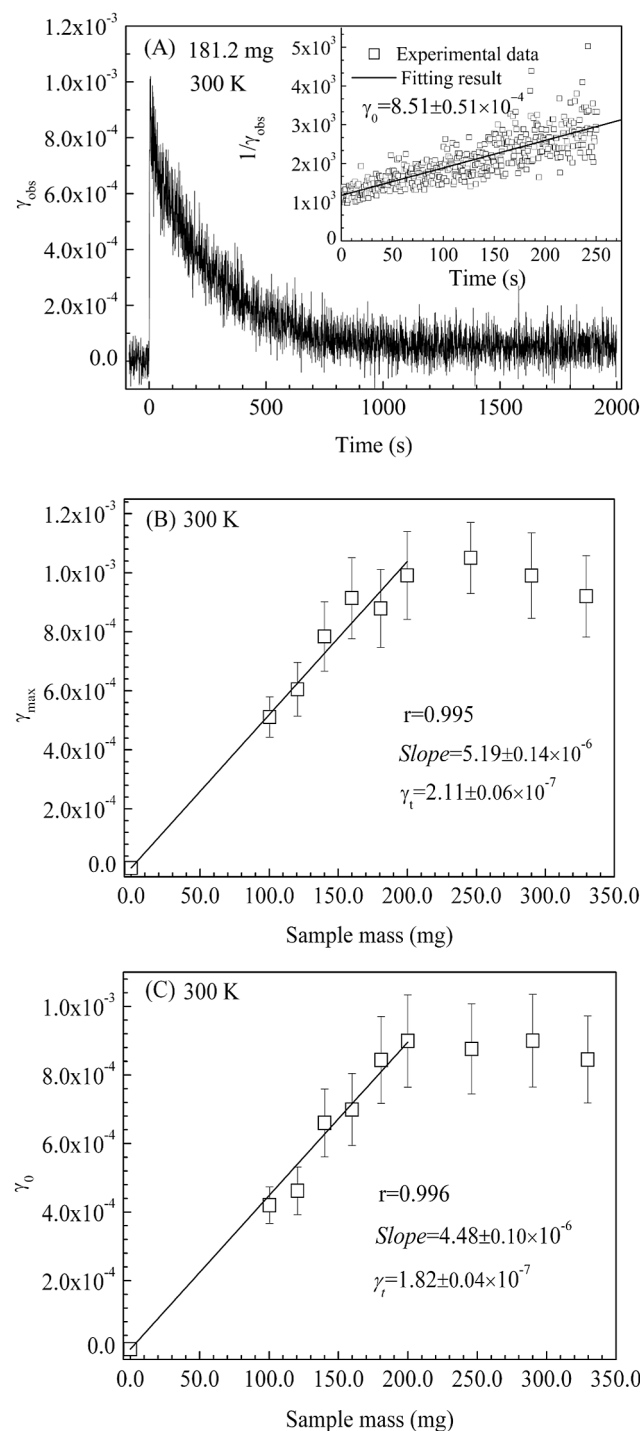

Figure 4. Uptake coefficients of OCS on kaolinite at 300 K and $(5.3 \pm 0.3) \times 10^{-6}$ Torr. (a) Changes in γ_{obs} with time; (b) changes in γ_{max} with sample mass; (c) changes in γ_0 with sample mass.

suggests a lower true uptake coefficient [*Underwood et al.*, 2000]. This phenomenon was in agreement with the measured small values of γ_t already mentioned. In this pressure region the average γ_t values based on γ_{max} and γ_0 were $(2.07 \pm 0.16) \times 10^{-7}$ and $(1.68 \pm 0.12) \times 10^{-7}$, respectively. Considering the higher reliability of γ_0, we conservatively
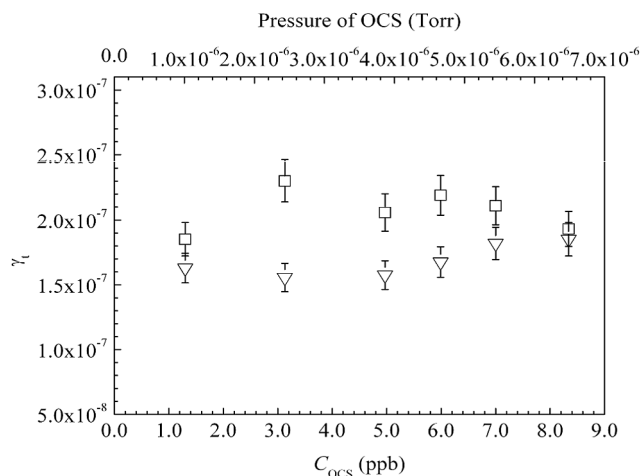
Table 1. Uptake Coefficients and Desorption Rate Constants at Different Temperatures

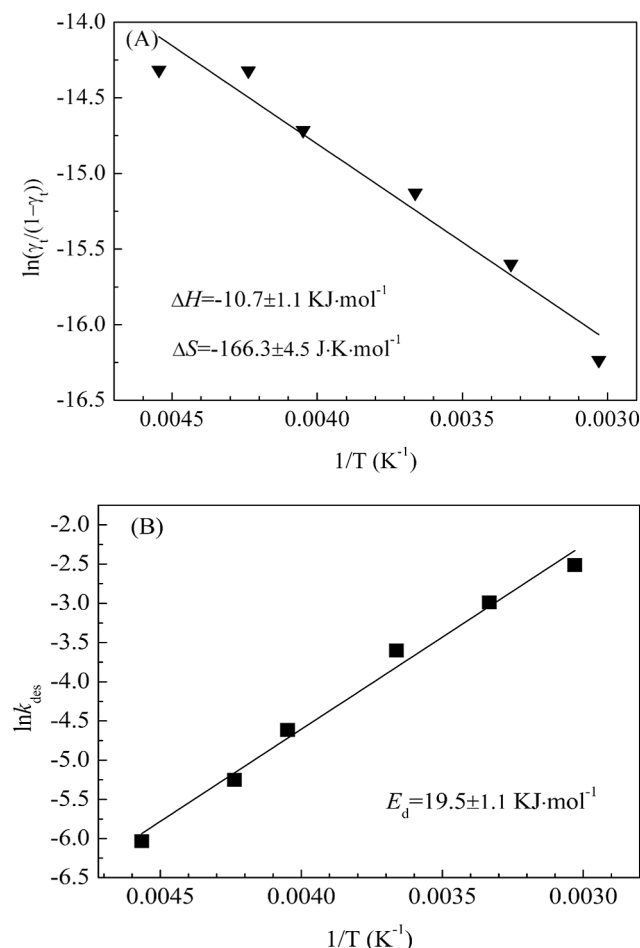| Temperature (K)	Γ		k_{des} ($\times 10^2$)
	γ_0(obs) ($\times 10^3$)	γ_t(BET) ($\times 10^7$)	
220	2.59 ± 0.39	6.06 ± 0.59	0.24 ± 0.02
236	2.58 ± 0.39	6.03 ± 0.60	0.52 ± 0.05
247	1.74 ± 0.26	4.07 ± 0.38	0.99 ± 0.09
273	1.15 ± 0.17	2.69 ± 0.25	2.73 ± 0.15
300	0.72 ± 0.11	1.68 ± 0.12	5.04 ± 0.23
330	0.38 ± 0.06	0.89 ± 0.08	8.10 ± 0.54

Figure 6. (a) Plot to determine ΔH and ΔS for OCS on kaolinite using the initial uptake coefficient; (b) dependence of desorption rate constant (k_{des}) on temperature. OCS pressure was $5.3 \pm 0.3 \times 10^{-6}$ Torr and sample mass was 181.2 mg.

the initial true uptake coefficient was in the range of $(8.90 \pm 0.81) \times 10^{-8} - (6.06 \pm 0.59) \times 10^{-7}$. Uptake coefficients decreased significantly with increasing temperature. This trend in the uptake coefficients with temperature agrees well with the physical adsorption process.

[20] Since the uptake coefficients showed a negative temperature dependence, the changes in observed enthalpy (ΔH_{obs}) and entropy (ΔS_{obs}) for OCS adsorption on kaolinite can be obtained by the following equation [*Jayne et al.*, 1991; *Hudson et al.*, 2002]:

$$\ln\left(\frac{\gamma_t}{1 - \gamma_t}\right) = -\frac{\Delta H_{obs}}{RT} + \frac{\Delta S_{obs}}{R}. \qquad (3)$$

Therefore, from a plot of the left side of equation (3) versus the inverse temperature, as shown in Figure 6a, the ΔH_{obs} and ΔS_{obs} were determined to be -10.7 ± 1.1 kJ mol^{-1} and -166.3 ± 4.5 J K^{-1} mol^{-1}, respectively. In Figure 6 the average uptake coefficients and desorption rate constants in Table 1 were used. The small ΔH_{obs} value also demon-

strates that OCS can only weakly adsorb on kaolinite. The empirical formula between the γ_t of OCS on kaolinite and temperature is given as

$$\gamma_t = \frac{\exp(1293/T - 20.0)}{1 + \exp(1293/T - 20.0)}, \qquad (4)$$

where T is temperature (K). Thus, the γ_t at other temperatures can be obtained using this equation.

[21] On the basis of the flux balance equation according to the uptake profiles shown in Figure 1a, the desorption rate constants can be calculated using the following equations [*Seisel et al.*, 2004, 2005; *Liu and He*, 2008]:

$$F_{des}(t) = k_{des} N_{ads}(t), \qquad (5)$$

$$F_{des}(t) = F(t)\left(1 + \frac{k_{ini}}{k_{esc}}\right) - F_0 \qquad (6)$$

where $F_{des}(t)$ is the desorption rate of OCS from the surface at time t (mol s^{-1}), k_{des} is the desorption rate constant (s^{-1}), $N_{ads}(t)$ is the number of adsorbed molecules on the surface, $F(t)$ is the flow out of the reactor at time t (mol s^{-1}), F_0 is the flow into the reactor (mol s^{-1}), k_{ini} is the initial rate constant and equals k_{ads} (s^{-1}), k_{esc} is the escape rate constant of Knudsen cell (s^{-1}), and $k_{esc} = \omega A_h$. The number of molecules adsorbed on the surface at time t, $N_{ads}(t)$, can be determined by integrating the QMS signal between $t = 0$ and the desired time t. The calculated k_{des} values are also listed in Table 1 and range from $(2.40 \pm 0.22) \times 10^{-3}$ to $(8.10 \pm 0.54) \times 10^{-2}$ s^{-1} with increasing temperature. The temperature dependence of k_{des} is shown in Figure 6b. According to the slope of this plot the activation energy for desorption (E_{des}) of OCS on kaolinite was calculated to be 19.5 ± 1.1 kJ mol^{-1}. The relatively low E_{des} value also confirms the weak adsorption of OCS on kaolinite.

4. Conclusions and Environmental Implications

[22] The uptake of OCS onto kaolinite was investigated within a temperature range of 220 to 330 K. Unlike the heterogeneous hydrolysis and oxidation taking place on Al_2O_3 and MgO, OCS can only reversibly adsorb at Al-OH sites on kaolinite in this temperature region. The percentage of reversibly adsorbed OCS increased from 12% (300 K) to 50% (238 K) with decreasing temperature.

[23] The initial true uptake coefficient showed no observable dependence on the pressure of OCS. It was measured to be $(1.68 \pm 0.12) \times 10^{-7}$ at 300 K. The initial true uptake coefficient varied significantly with temperature, and it can be expressed as equation (4). Based on the temperature dependence of uptake coefficients, ΔH_{obs} and ΔS_{obs} during the adsorption process were -10.7 ± 1.1 kJ mol^{-1} and -166.3 ± 4.5 J K^{-1} mol^{-1}, respectively. The activation energy for desorption of OCS on kaolinite was 19.5 ± 1.1 kJ·mol^{-1}. The relatively low values of ΔH_{obs} and E_{des} also demonstrate the weak adsorption process taking place on kaolinite.

[24] The initial uptake coefficients of OCS on kaolinite at 300 K are less than about one half of those on α-Al_2O_3 and

MgO [*Liu and He*, 2008; *Liu et al.*, 2009]. In addition, the uptake of OCS on α-Al_2O_3 and MgO includes heterogeneous hydrolysis and oxidation processes, while only adsorption takes place on kaolinite. Therefore, it can be concluded that the contribution of uptake by kaolinite to the sinks of OCS in the troposphere is less important than those of α-Al_2O_3 and MgO.

[25] The lifetime of OCS owing to uptake onto kaolinite can be estimated by

$$\tau = \frac{4}{\gamma_t \bar{v} SA}, \tag{7}$$

where $\bar{v}$ is the average velocity of OCS (m s^{-1}), γ_t is the initial true uptake coefficient at 300 K, and SA is the surface area of the dust event (m^2·m^{-3}). However, the flux of OCS owing to uptake onto kaolinite cannot be estimated accurately, as the loading of kaolinite in atmospheric particles is unavailable. If we assume that all mineral dust is in the form of kaolinite, and the dust loading is 150 μm^2 cm^{-3} [*de Reus et al.*, 2000; *Frinak et al.*, 2004] under extreme conditions, the lifetime of OCS owing to heterogeneous uptake onto kaolinite is calculated to be 16.5 years. This value is much higher than the average lifetime of OCS (4.3 years) in the troposphere [*Chin and Davis*, 1995], which means that the contribution of kaolinite to the sink of OCS is limited in the atmosphere even under extreme conditions. It should be noted, however, that the γ_t value at the lower temperature should increase significantly. For example, at 180 K the γ_t value should equal 2.70×10^{-6} (extrapolated from equation (4)). Using this value, the lifetime of OCS on kaolinite is calculated to be 1.2 years. Kaolinite may, therefore, influence the local concentration of OCS, especially in very low temperature regions with a high concentration of kaolinite.

[26] Furthermore, soils were identified as being very important in the sinks and sources of OCS in the atmosphere [*Kesselmeier et al.*, 1999; *Kettle et al.*, 2002; *Liu et al.*, 2007a; *Yi et al.*, 2007]. Oxic soils, for example, are considered important sinks of OCS, whereas anoxic soils are sources of OCS. Studies have shown that the consumption of OCS by oxic soils or the production of OCS by anoxic soils is related to microbial and chemical processes [*Kesselmeier et al.*, 1999; *Conrad*, 1996]. As adsorption and desorption are the primary steps related to microbial and chemical processes, the reversible adsorption characteristic confirmed in this study should be favored by both the consumption of OCS by oxic soils and the release of OCS by anoxic soils.

References

Al-Abadleh, H. A., and V. H. Grassian (2000), Heterogeneous reaction of NO$_2$ on hexane soot: A Knudsen cell and FT-IR study, *J. Phys. Chem. A*, *104*, 11,926–11,933.

Andreae, M. O., and P. J. Crutzen (1997), Atmospheric aerosols: Biogeochemical sources and role in atmospheric chemistry, *Science*, *276*, 1052–1058.

Angelini, M. M., R. J. Garrard, S. J. Rosen, and R. Z. Hinrichs (2007), Heterogeneous reactions of HNO$_3$ and NO$_2$ on the clay minerals kaolinite and pyrophyllite, *J. Phys. Chem. A*, *111*, 3326–3335.

Beichert, P., and B. J. Finlayson-Pitts (1996), Knudsen cell studies of the uptake of gaseous HNO$_3$ and other oxides of nitrogen on solid NaCl: The role of surface-adsorbed water, *J. Phys. Chem.*, *100*, 15,218–15,228.

Carlos-Cuellar, S., P. Li, A. P. Christensen, B. J. Krueger, C. Burrichter, and V. H. Grassian (2003), Heterogeneous uptake kinetics of volatile organic compounds on oxide surfaces using a Knudsen cell reactor: Adsorption of acetic acid, formaldehyde, and methanol on α-Fe$_2$O$_3$, α-Al$_2$O$_3$ and SiO$_2$, *J. Phys. Chem. A*, *107*, 4250–4261.

Chen, H. H., L. D. Kong, J. M. Chen, R. Y. Zhang, and L. Wang (2007), Heterogeneous uptake of carbonyl sulfide on hematite and hematite-NaCl mixtures, *Environ. Sci. Technol.*, *41*, 6484–6490.

Chin, M., and D. D. Davis (1995), A reanalysis of carbonyl sulfide as a source of stratospheric background sulfur aerosol, *J. Geophys. Res.*, *100*(DS), 8993–9005.

Conrad, R. (1996), Soil microorganisms as controller of atmospheric trace gases (H$_2$, CO, CH$_4$, OCS, N$_2$O and NO), *Microbiol. Rev.*, *60*(4), 609–640.

Crutzen, P. J. (1976), The possible importance of CSO for the sulfate layer of the stratosphere, *Geophys. Res. Lett.*, *3*, 73–76.

Dentener, F. J., G. R. Carmichael, Y. Zhang, J. Lelieveld, J., and P. J. Crutzen (1996), Role of mineral aerosol as a reactive surface in the global troposphere, *J. Geophys. Res.*, *101*, 22,869–22,889.

de Reus, M., F. Dentener, A. Thomas, S. Borrmann, J. Ström, and J. Lelieveld (2000), Airborne observations of dust aerosol over the North Atlantic Ocean during ACE 2: Indications for heterogeneous ozone destruction, *J. Geophys. Res.*, *105*, 15,263–15,275.

Frinak, E. K., S. J. Wermeille, C. D. Mashburn, M. A. Tolbert, and C. J. Pursell (2004), Heterogeneous reaction of gaseous nitric acid on γ–phase iron(III) oxide, *J. Phys. Chem. A*, *108*, 1560–1566.

Gebel, M. E., and B. J. Finlayson-Pitts (2001), Uptake and reaction of ClONO$_2$ on NaCl and synthetic sea salt, *J. Phys. Chem. A*, *105*, 5178–5187.

Greshake, A., W. Klöck, P. Arndt, M. Maetz, G. J. Flynn, S. Bajt, and A. Bischoff (1998), Heating experiments simulating atmospheric entry heating of micrometeorites: clues to their parent body sources, *Meteor. Planet Sci.*, *33*, 267–290.

Hanisch, F., and J. N. Crowley (2001), The heterogeneous reactivity of gaseous nitric acid on authentic mineral dust samples, and on individual mineral and clay mineral components, *Phys. Chem. Chem. Phys.*, *3*, 2474–2482.

Hatch, C. D., R. V. Gough, O. B. Toon, and M. A. Tolbert (2008), Heterogeneous nucleation of nitric acid trihydrate on clay minerals: Relevance to type Ia polar stratospheric clouds, *J. Phys. Chem. B*, *112*, 612–620.

He, H., J. F. Liu, Y. J. Mu, Y. B. Yu, and M. X. Chen (2005), Heterogeneous oxidation of carbonyl sulfide on atmospheric particles and alumina, *Environ. Sci. Technol.*, *39*, 9637–9642.

Hudson, P. K., J. E. Shilling, M. A. Torlbert, and O. B. Toon (2002), Uptake of nitric acid on ice at tropospheric temperatures: Implications for cirrus clouds, *J. Phys. Chem. A*, *106*, 9874–9882.

Jacob, D. J. (2000), Heterogeneous chemistry and tropospheric ozone, *Atmos. Environ.*, *34*, 2131–2159.

Jayne, J. T., X. S. Duan, P. Davidovits, D. R. Worsnop, M. S. Zahniser, and C. E. Kolb (1991), Uptake of gas-phase alcohol and organic acid molecules by water surfaces, *J. Phys. Chem.*, *95*, 9329–6336.

Kesselmeier, J., N. Teusch, and U. Kuhn (1999), Controlling variables for the uptake of atmospheric carbonyl sulfide by soil, *J. Geophys. Res.*, *104*(D9), 11,577–11,584.

Kettle, A. J., U. Kuhn, M. von Hobe, J. Kesselmeier, and M. O. Andreae (2002), Global budget of atmospheric carbonyl sulfide: Temporal and spatial variations of the dominant sources and sinks, *J. Geophys. Res.*, *107*(D22), 4658, doi:10.1029/2002JD002187.

Liu, J. F., Y. B. Yu, Y. J. Mu, and H. He (2006), Mechanism of heterogeneous oxidation of carbonyl sulfide on Al$_2$O$_3$: An in situ diffuse reflectance infrared Fourier transform spectroscopy investigation, *J. Phys. Chem. B*, *110*, 3225–3230.

Liu, J. F., Y. J. Mu, C. M. Geng, Y. B. Yu, H. He, and Y. H. Zhang (2007) Uptake and conversion of carbonyl sulfide in a lawn soil, *Atmos. Environ.*, *41*, 5697–5706.

Liu, Y. C., and H. He (2008), Temperature dependence of heterogeneous reaction of carbonyl sulfide on magnesium oxide, *J. Phys. Chem. A*, *112*, 2820–2826.

Liu, Y. C., and H. He (2009), Experimental and theoretical study of hydrogen thiocarbonate for heterogeneous reaction of carbonyl sulfide on magnesium oxide, *J. Phys. Chem. A*, *113*, 3387–3394.

Liu, Y. C., H. He, W. Q. Xu, and Y. B. Yu (2007), Mechanism of heterogeneous reaction of carbonyl sulfide on magnesium oxide, *J. Phys. Chem. A*, *111*, 4333–4339.

Liu, Y. C., H. He, and J. Y. Mu (2008), Heterogeneous reactivity of carbonyl sulfide on α-Al$_2$O$_3$ and γ-Al$_2$O$_3$, *Atmos. Environ.*, *42*, 960–969.

Liu, Y. C., Q. X. Ma, and H. He (2009), Comparative study of effect of water on the heterogeneous reactions of carbonyl sulfide on the surface of α-Al$_2$O$_3$ and MgO, *Atmos. Chem. Phys.*, *9*, 6273–6286.

Parry, E. P. (1963), An infrared study of pyridine absorbed or acidic solids. Characterization of surface acidity, *J. Catal.*, *2*, 371–379.

Seisel, S., Y. Lian, T. Keil, M. E. Trukhin, and R. Zellner (2004), Kinetics of the interaction of water vapour with mineral dust and soot surfaces at *T* = 298 K, *Phys. Chem. Chem. Phys.*, *6*, 1926–1932.

Seisel, S., A. Pashkova, Y. Lian, and R. Zellner (2005), Water uptake on mineral dust and soot: A fundamental view of the hydrophilicity of atmospheric particles?, *Faraday Discuss.*, *130*, 437–451.

Simmons, J. S., L. Klemedtsson, H. Hultberg, and M. E. Kines (1999), Consumption of atmospheric carbonyl sulfide by coniferous boreal forest soils, *J. Geophys. Res.*, *104*(D9), 11,569–11,576.

Smith, I. W. M. (2003), Laboratory studies of atmospheric reactions at low temperatures, *Chem. Rev.*, *103*, 4549–4564.

Tabor, K., L. Gutzwiller, and M. J. Rossi (1994), Heterogeneous chemical kinetics of NO$_2$ on amorphous carbon at ambient temperature, *J. Phys. Chem. A*, *98*, 6172–6186.

Turco, R. P., R. C. Whitten, O. B. Toon, J. B. Pollack, and P. Hamill (1980), OCS, stratospheric aerosols and climate, *Nature*, *283*, 283–286.

Ullerstam, M., M. S. Johnson, R. Vogt, and E. Ljungström (2003), DRIFTS and Knudsen cell study of the heterogeneous reactivity of SO$_2$ and NO$_2$ on mineral dust, *Atmos. Chem. Phys.*, *3*, 2043–2051.

Underwood, G. M., P. Li, C. R. Usher, and V. H. Grassian (2000), Determining accurate kinetic parameters of potentially important heterogeneous atmospheric reactions on solid particle surfaces with a Knudsen cell reactor, *J. Phys. Chem. A*, *104*, 819–829.

Underwood, G. M., P. Li, H. A. Al-Abadleh, and V. H. Grassian (2001), A Knudsen cell study of the heterogeneous reactivity of nitric acid on oxide and mineral dust particles, *J. Phys. Chem. A*, *105*, 6609–6620.

Usher, C. R., A. E. Michel, and V. H. Grassian (2003), Reactions on mineral dust, *Chem. Rev.*, *103*, 4883–4939.

Watts, S. F. (2000), The mass budgets of carbonyl sulfide, dimethyl sulfide, carbon disulfide and hydrogen sulfide, *Atmos. Environ.*, *34*, 761–799.

Wu, H. B., X. Wang, J. M. Cheng, H. K. Yu, H. X. Xue, X. X. Pan, and F. Q. Hou (2004), Mechanism of the heterogeneous reaction of carbonyl sulfide with typical components of atmospheric aerosol, *Chin. Sci. Bull.*, *49*, 739–743.

Wu, H. B., X. Wang, and J. M. Cheng (2005), Photooxidation of carbonyl sulfide in the presence of the typical oxides in atmospheric aerosol, *Sci. China. Ser. B Chem.*, *48*, 31–37.

Yi, Z. G., X. M. Wang, G. Y. Sheng, D. Q. Zhang, G. Y. Zhou, and J. M. Fu (2007), Soil uptake of carbonyl sulfide in subtropical forests with different successional stages in south China, *J. Geophys. Res.*, *112*, D08302, doi:10.1029/2006JD008048.

H. He, C. Liu, Y. Liu, and J. Ma, State Key Laboratory of Environmental Chemistry and Ecotoxicology, Research Center for Eco-Environmental Sciences, Chinese Academy of Sciences, Beijing 100085, China. (honghe@ rcees.ac.cn)